

Robot-assisted Microsurgical Forceps with Haptic Feedback for Transoral Laser Microsurgery

Nikhil Deshpande, Manish Chauhan, Claudio Pacchierotti, Domenico Prattichizzo,
Darwin G. Caldwell, and Leonardo S. Mattos

Department of Advanced Robotics, Istituto Italiano di Tecnologia (IIT), Via Morego 30, Genova, 16163, Italy
Email: {nikhil.deshpande, manish.chauhan, claudio.pacchierotti, domenico.prattichizzo,
darwin.caldwell, leonardo.mattos}@iit.it

Abstract—In this paper, a novel, motorized, multi-degrees-of-freedom (DoF), microsurgical forceps tool is presented, which is based on a master-slave teleoperation architecture. The slave device is a 7-DoF manipulator with: (i) 6-DoF positioning and orientation, (ii) 1 open/close gripper DoF; and (iii) an integrated force/torque sensor for tissue grip-force measurement. The master device is a 7-DoF haptic interface which teleoperates the slave device, and provides haptic feedback in its gripper interface. The combination of the device and the surgeon interface replaces the manual, hand-held device providing easy-to-use and ergonomic tissue control, simplifying the surgical tasks. This makes the system suitable to real surgical scenarios in the operating room (OR). The performance of the system was analysed through the evaluation of teleoperation control and characterization of gripping force. The new system offers an overall positioning error of less than $400 \mu\text{m}$ demonstrating its safety and accuracy. Improved system precision, usability, and ergonomics point to the potential suitability of the device for the OR and its ability to advance haptic-feedback-enhanced transoral laser microsurgeries.

Index Terms—microsurgical forceps, robot-assisted, haptic interface, transoral laser microsurgeries

I. INTRODUCTION

Robot-assisted surgical systems are increasingly becoming an accepted component of the state-of-the-art operating room (OR). This is due not only to the significant advantages they bring for surgery, such as increased precision, reduced instrument tremors, error-free and timely execution of repetitive tasks, etc., but also due to the improvements they bring for the surgeons themselves, with ease-of-use, comfort, and importantly, improved perception of the surgical site through high-resolution visualization and haptic feedback [1], [2]. This is especially true in the case of microsurgeries, such as transoral microsurgery, where the surgical areas are small (in the order of mm). Transoral Laser Microsurgery (TLM) is a form of minimally invasive surgery which deals with the treatment of laryngeal and other head-and-neck malignancies, e.g., cysts, polyps, and tumours. The CO_2 surgical laser coupled with a surgical microscope is one of the main tools in TLM. A mechanical micromanipulator joystick is used by the surgeon to manually aim the laser beam for incisions at the surgical site from outside the mouth, as seen in Fig. 1. Microsurgical forceps are used for tissue manipulation, and a footswitch serves to activate the laser when desired.

Considering the large operating distance (typically between 250 to 400 mm) and a small surgical area (typically $40 \times 40 \text{ mm}^2$), to perform precise surgery with optimal outcome, the surgeons are required to be highly skilled to overcome challenges of: (i) poor operating ergonomics, (ii) difficult hand-eye-foot coordination, (iii) manual, coordinated control of the tools for manipulation and incision of tissue, and (iv) lack of haptic perception added to the inadequate arm support and uncomfortable wrist excursions.

Earlier research by the authors resulted in improved computer-assisted systems for TLM with a novel surgeon-machine interface (“Virtual Microscope” system [3]) providing: (i) precise teleoperated laser aiming through an easy-to-use stylus tablet, (ii) improved ergonomics for high-

resolution visualization and laser activation, and (iii) assistive intraoperative features for surgical enhancement. This paper extends the benefits of such robot-assisted technologies to the aspect of tissue manipulation using an ergonomic interface with haptic feedback. Haptic feedback is considered valuable for teleoperated surgical procedures, showing enhanced surgeon performance through improved perception accuracy, decreased completion time, and decreased peak and mean applied forces, in a wide range of applications [4], [5], [6]. These benefits lend themselves readily towards facilitating and improving the complex suite of otolaryngological techniques involved in TLM.

The new robot-assisted microsurgical forceps design replaces the traditional, hand-held, manual tool with a teleoperation system: (i) a 7 degree-of-freedom (DoF) microsurgical forceps manipulator; (ii) a 7-DoF teleoperation haptic master interface, the *Force Dimension Omega.7*; and (iii) an integrated force/torque sensor for haptic feedback, the ATI Nano17. The concept is shown in Fig. 2. Robot-assisted surgical instruments for transoral surgery have been a subject

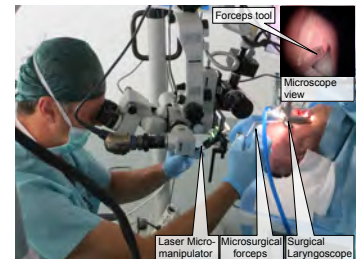


Fig. 1. Traditional TLM setup showing intraoperative use of microsurgical forceps

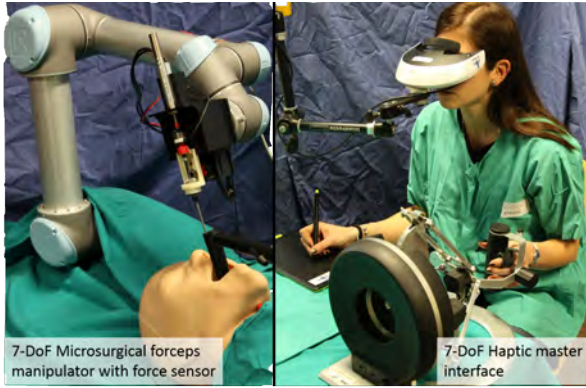


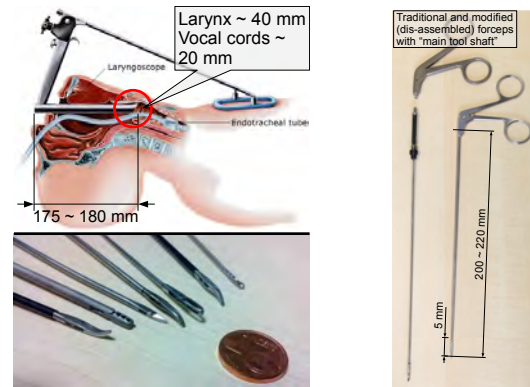
Fig. 2. Robot-assisted microsurgical forceps concept

of extensive research [7], [8], [9]. Yet, they are mainly focused on cold-steel instrument-based surgery and not TLM. The typical instrument shaft diameter in cold-steel surgeries is 3 mm and higher, while in TLM, the tools are typically around 2 mm in diameter. Maier et al. [10] presented an effective solution with a lightweight manipulator to which standard surgical tools can be attached directly without any modification. This meant that typical tool-shafts of ϕ 2 mm could be directly used allowing a common interface for the surgeon irrespective of the tool. The developments in this paper are inspired by the approach of having a common interface for the surgeon, with added features and haptic feedback to improve their usability, accuracy, and safety.

II. HARDWARE DESIGN

In the state-of-the-art TLM procedure, a laryngoscope is used to expose the surgical site allowing direct line-of-sight for the surgical microscope, as seen in Fig. 1. The laryngoscope has a length of 180 mm and a cross-section of 17 mm (Fig. 3a) [9]. Microsurgical tools, e.g., forceps, are manually operated through the laryngoscope and help the surgeons in: (i) exposure of surgical site pathology; (ii) tissue manipulation; (iii) tissue palpation; and (iv) orienting the tissue to be perpendicular to the laser path, in traction (stretched), for precise cuts with minimal thermal damage (Fig. 1).

State-of-the-art microsurgical forceps are long and rigid, with an average shaft length of about 200-220 mm. The tool-shaft cross-section is about 2 - 3 mm and they are usually pre-curved to the left or right for accessing the two sides of the larynx, as seen in Fig. 3. These manual tools are single purpose and available with only 1 DoF (open/close). The TLM surgical area, the larynx, is a highly restricted space, varying from about 45 mm (diagonal length, males) to about 25 mm (females), reducing further to about 11 - 21 mm in the vocal cord region [11]. The procedure therefore, demands a great level of accuracy and dexterity for coordinated bimanual control to guarantee total pathology removal. The research in this paper addresses these issues by redesigning the surgeon interface for tissue manipulation. In the redesign, the tool shaft and gripper of the traditional forceps are used and proximal mechanisms are introduced.



(a) Anatomical dimensions and tool variety in TLM (b) Microsurgical forceps dimensions

Fig. 3. Microsurgical anatomy and tools in TLM

A. Redesign of existing microsurgical forceps

The adopted modular architecture gives a common surgeon interface with interchangeability of commonly used tool-tips in TLM (Fig. 3a). The motorized microsurgical forceps with an additional rotational DoF shall allow: (i) gripping-n-turning of tissue for better surgical exposure; and (ii) improving the surgical access to different parts of the larynx. Existing TLM microsurgical forceps were reconfigured into three modules: (i) Main tool shaft; (ii) Mechanism housing; and (iii) Actuator housing.

1) *Main Tool Shaft (mts)*: This component consists of an outer shaft (ϕ 2.5 mm) and an inner translating wire (*itw*, ϕ 1 mm) for the open/close DoF (Fig. 4). The distal end of the *mts* consists of a dual-jaw gripper with ϕ 2 mm and length of 5 mm. Two adaptations are introduced at the proximal end of the *mts*: (i) a hollow M6 grub screw is attached to the outer shaft; and (ii) an extension bar (~ 31 mm) with an M3 screw are attached to the *itw*.

2) *Mechanism housing (mh)*: This component houses the mechanisms for the original open/close DoF and the newly introduced rotational DoF (Fig. 5). Along with the links and connectors to the sensors/actuators, the housing consists of:

- 1) Rotational DoF: An anti-backlash, hollow, miter gear assembly (Nordex LHS E2-30) provides the rotation of the *mts*. The M6 grub screw of the *mts* fits into an M6 brass-insert fixed to the axial miter gear. The *itw* is made to pass through this axial miter gear. The normal miter gear couples to the rotary actuator.

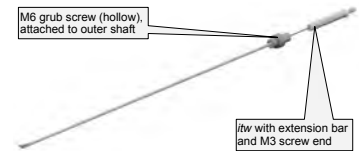


Fig. 4. Main tool shaft - adaptations



Fig. 5. Mechanism housing

2) Open/Close DoF: The *itw* is attached to a “sliding cylinder assembly” (*sca*) through an M3 brass-insert. The *sca* includes an internal bearing to allow free rotation of the *itw* with the rotational DoF. The distal end of the *sca* couples to the linear actuator.

3) *Actuator housing (ah)*: This component houses the two actuators used for the two DoFs (Fig. 6). A linear actuator (CAL12 series) is used for the open/close DoF and is coupled with the *sca*. A rotary motor (Maxon GM20) provides the rotational DoF through its coupling with the miter gear assembly in *mh*.



Fig. 6. 2-DoF motorized microsurgical forceps assembled with actuator housing

B. 7-DoF manipulator: Integration of forceps with a robotic manipulator and force/torque sensor

The motorized microsurgical forceps assembly is attached to a 6-DoF robotic manipulator, the Universal Robots UR5, and integrated with the 6-axis force/torque sensor, the ATI Nano17, to form the 7-DoF microsurgical forceps manipulator, as shown in Fig. 2.

- 1) The UR5 has a payload capacity of 5 kg, a repeatability of 0.1 mm with a reach radius of 850 mm, and can be controlled at 125 Hz. These values make it suitable for precise applications such as TLM. The 2-DoF microsurgical forceps are attached to the end-effector wrist of the UR5 at a 90° angle. Since the microsurgical forceps already has a rotational DoF, the final wrist DoF of the UR5 is unused. The Denavit-Hartenberg parameters for the device are suitably updated to operate as a 7-DoF manipulator.
- 2) The ATI Nano17 Force/Torque sensor provides six-dimensional signal components (both forces and torques) in a small footprint ($\phi = 17$ mm, $L = 14.5$ mm). The sensor offers a resolution as low as 3.125 mN with a rated force sensing of up to 70 N and torque sensing up to 500 Nmm. It registers data at > 2 kHz. For haptic feedback, the sensor is located as part of the *sca* in *mh*, with the z-axis of the sensor axially coincident with the *itw*, as seen in Fig. 5. The closing of the gripper jaws on tissue produces a reaction force which is transmitted to the surface of the sensor as a pull/push force. The sensor thus outputs a signal corresponding to this pull/push force, which is in direct proportion to the actual tissue gripping force.
- 3) Finally, the haptic master interface, the 7-DoF *Force Dimension Omega.7*, is used to teleoperate this 7-DoF robotic forceps manipulator (Fig. 2). The three translating DoFs are *active* implying possibility for haptic feedback, while the three rotational DoFs are *passive*. The interface is also equipped with an active gripper, the 7th DoF.

III. CONTROL DESIGN

The 2-DoF motorized microsurgical forceps are controlled through a custom designed motor control board, based on the TI-LM3S microcontroller. Custom PID control code allows both position and velocity-based control of the actuators. The *Omega.7* interface was used as an impedance haptic device. The measured position of the haptic end-effector sets the reference target position for the microsurgical forceps gripper. The device allows gesture scaling and tremor suppression between the master and slave environments. The haptic control loop runs at 2 kHz.

A. Motion Control

The velocities of the robotic manipulator joints $\dot{q} \in \mathbb{R}^6$ can be expressed as:

$$\dot{\mathbf{q}}_r = \mathbf{J}^{-1} \dot{\mathbf{q}}_h \zeta \quad (1)$$

where \mathbf{J}^{-1} is the inverse of the manipulator Jacobian matrix $\mathbf{J} \in \mathbb{R}^{6 \times 6}$ and $\dot{\mathbf{q}}_h \in \mathbb{R}^6$ are the velocities of the *Omega.7*'s end-effector. The $\dot{\mathbf{q}}_h$ velocities of the haptic end-effector are scaled through a low-pass filter in (2), with a tunable factor β to control the level of high-frequency tremor suppression.

$$\dot{\mathbf{q}}_h^k = (1 - \beta) \cdot \dot{\mathbf{q}}_h^{k-1} + \beta \cdot \dot{\mathbf{q}}_h^{encoder} \quad (2)$$

The gesture scaling factor ζ is tunable to allow coarse and fine gestures in different stages of operation. For instance, a value of 0.2 in all directions implies that moving the haptic end-effector by 10 cm would move the forceps gripper's reference position by 2 cm. The speed of motion is also controlled simultaneously.

The integrated system uses a dedicated Gigabit Ethernet connection between the master and slave devices, ensuring minimal time delay between the two. A time-domain, two-layer, passivity controller [12] preserves the stability. Its top layer, *Transparency Layer*, allows desired transparency between master-&-slave, while the lower, *Passivity Layer*, ensures the passivity of the system. The *Omega.7*'s gripper DoF is mapped directly to the open/close DoF of the microsurgical forceps through simple position control.

IV. EVALUATION AND DISCUSSION

The performance of the motion control and the variance in the haptic gripping force were evaluated through characterization trials.

A. Motion control evaluation

The surgeon shall be controlling the microsurgical forceps while simultaneously visualizing the actions through visual feedback of the surgical site, making it a human-in-the-loop feedback system. The gestures of the surgeon on the haptic master interface are directly mapped to the slave environment, allowing for any positioning and orientation corrections in real time.

The evaluation characterized the relationship expressed in (1), i.e., how well the slave replicates the master motion.

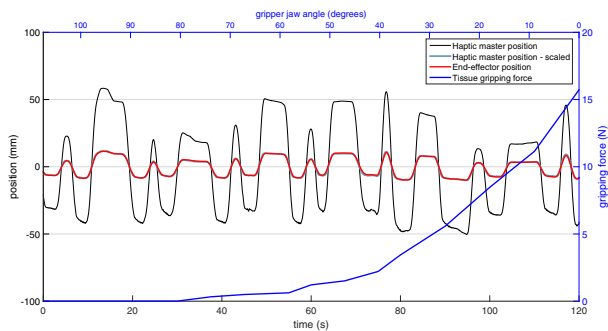


Fig. 7. Motion control and tissue gripping force evaluation

The haptic master interface was moved in free-space over a period of 120 seconds and the positions of the slave device were recorded. Figure 7 shows a representative graph for a evaluation for a single axis of the end-effector. A gesture scaling factor of $\zeta = 0.2$ was used for the evaluation. As can be seen, the slave device is able to track the gestures of the master interface very well. The overall error, over the 120 seconds, in the 3-axis positioning of the slave device end-effector was found to be **0.3901 mm** (RMSE) with a standard deviation of **0.3829 mm**. The position mapping error is therefore less than $400 \mu\text{m}$.

B. Haptic feedback characterization

The levels of tissue gripping force vary with the amount of gripping on the tissue, i.e., the angle that the jaws of the gripper are closed. An independent evaluation was made to quantify the haptic force to be fed back to the haptic master interface. Using a high-precision X-Y table (Siskiyou 1620-XYZR) the closing angle of the forceps gripper jaws was precisely controlled (with a resolution of $\sim 1^\circ$) and the sensor output signal was recorded for different angles of the jaws, i.e., different values of pull/push force on the sensor. Ex-vivo chicken tissue samples (min. $40 \times 40 \text{ mm}^2$ area and 5 mm thickness) were used for the trials. For every angular position of the gripper jaw the sensor values were averaged over 5 trials with 5 different tissue samples. As seen from Fig. 7, the gripping force increases non-linearly from the fully-open position of the gripper jaws ($\sim 80^\circ$, the tissue not touching the jaws) to the fully-closed position (indicated as 0°). A maximum gripping force of about 16 N was noted from these trials. As noted in [13], gripping force values between 6 and 16 N are sufficient for grasping and maneuvering tissue. This information is helpful in defining the range of gripping forces involved and sizing the robotic actuator to be used for the gripping action.

V. CONCLUSIONS AND FUTURE WORK

This paper presented a novel design of a modular, integrated, multi-DoF, motorized microsurgical forceps tool for intraoperative use in transoral laser microsurgeries. The new design replaces the traditional, hand-held, manual tool with a teleoperation system consisting of: (i) a 7 DoF microsurgical forceps manipulator; (ii) a 7-DoF teleoperation haptic master interface; and (iii) an integrated force/torque sensor for haptic

feedback of the tissue gripping force. The system provides: (i) improved precision, safety, and controllability with a positioning error less than $400 \mu\text{m}$; (ii) enhanced surgical site perception with haptic feedback which can be tuned suitably based on surgical preferences; and (iii) intuitive and ergonomic operation of the microsurgical forceps with a common surgeon interface providing gesture scaling and overcoming the problems of hand tremors and wrist excursions. The developments presented here, integrated with the “Virtual Microscope” system from [3] shall lead to a holistic, robot-assisted surgical system for TLM, enhancing the capacity for safer minimally invasive microsurgeries, requiring delicate and precise actions.

In the extension of this research, the evaluation of the new tool with user trials shall be investigated. These shall provide a comparative performance analysis against the traditional forceps tool, as well as an understanding of the preferred modality and utility of gripping force feedback for the surgeons. The ultimate goal is to evaluate the robustness and safety of the mechanism making it system advantageous in the real surgical scenario.

REFERENCES

- [1] M. D. O’Toole, K. Bouazza-Marouf, D. Kerr, M. Goorochurn, and M. Vloeberghs, “A Methodology for Design and Appraisal of Surgical Robotic Systems,” *Robotica*, vol. 28, pp. 297–310, 2010.
- [2] C. W. Kennedy, T. Hu, J. P. Desai, A. S. Wechsler, and J. Y. Kresh, “A novel approach to robotic cardiac surgery using haptics and vision,” *Cardiovascular Engineering*, vol. 2, no. 1, pp. 15–22, 2002.
- [3] N. Deshpande, J. Ortiz, D. G. Caldwell, and L. S. Mattos, “Enhanced computer-assisted laser microsurgeries with a “Virtual Microscope” based surgical system,” in *Proc. Intl. Conf. on Robotics and Automation, (ICRA 2014)*, 2014, pp. 4194–4199.
- [4] A. M. Okamura, “Methods for haptic feedback in teleoperated robot-assisted surgery,” *Industrial Robot: An International Journal*, vol. 31, no. 6, pp. 499–508, 2004.
- [5] O. Van der Meijden and M. Schijven, “The value of haptic feedback in conventional and robot-assisted minimal invasive surgery and virtual reality training: a current review,” *Surgical Endoscopy*, vol. 23, no. 6, pp. 1180–1190, 2009.
- [6] C. Pacchierotti, L. Meli, F. Chinello, M. Malvezzi, and D. Prattichizzo, “Cutaneous haptic feedback to ensure the stability of robotic teleoperation systems,” *International Journal of Robotics Research*, vol. 34, no. 14, pp. 1773–1787, 2015.
- [7] N. Simaan, R. Taylor, and P. Flint, “A Dexterous System for Laryngeal Surgery,” in *Proc. Intl. Conf. on Robotics and Automation, (ICRA 2004)*, 2004, pp. 351–357.
- [8] C. He, K. Olds, I. Iordachita, and R. Taylor, “A New ENT Microsurgery Robot: Error Analysis and Implementation,” in *Proc. Intl. Conf. on Robotics and Automation, (ICRA 2013)*, 2013, pp. 1221–1227.
- [9] S. Wang, Q. Li, J. Ding, and Z. Zhang, “Kinematic Design for Robot-assisted Laryngeal Surgery Systems,” in *Proc. IEEE/RSJ Intl. Conf. on Intelligent Robots and Systems (IROS 2006)*, 2006, pp. 2864–2869.
- [10] T. Maier, G. Strauss, M. Hofer, T. Kraus, A. Runge, R. Stenzel, J. Gumprecht, T. Berger, A. Dietz, and T. C. Lueth, “A New Micromanipulator System for Middle-Ear Surgery,” in *Proc. Intl. Conf. on Robotics and Automation, (ICRA 2010)*, 2010, pp. 1568–1573.
- [11] M. Hirano, “Morphological Structure of the Vocal Cord as a Vibrator and its Variations,” *Folia Phoniatrica et Logopaedica*, vol. 26, pp. 89–94, 1974.
- [12] M. Franken, S. Stramigioli, S. Misra, C. Secchi, and A. Macchelli, “Bilateral telemanipulation with time delays: a two-layer approach combining passivity and transparency,” *IEEE Transactions on Robotics*, vol. 27, no. 4, pp. 741–756, 2011.
- [13] H. Yamanaka, K. Makiyama, K. Osaka, M. Nagasaka, M. Ogata, T. Yamada, and Y. Kubota, “Measurement of the Physical Properties during Laparoscopic Surgery Performed on Pigs by Using Forceps with Pressure Sensors,” *Advances in Urology*, vol. 495308, 2015.